APPLIED PHYSICS LETTERS **88**, 182508 (2006)

Effect of film roughness in MgO-based magnetic tunnel junctions

Weifeng Shen,[a] Dipanjan Mazumdar, and Xiaojing Zou
Physics Department, Brown University, Providence, Rhode Island 02912

Xiaoyong Liu and B. D. Schrag
Micro Magnetics, Inc., Fall River, Massachusetts 02720

Gang Xiao
Physics Department, Brown University, Providence, Rhode Island 02912

(Received 23 February 2006; accepted 22 March 2006; published online 5 May 2006)

We have systematically investigated the dependence of tunnel magnetoresistance in MgO-based magnetic tunnel junctions as a function of Ar pressure during sputtering. The MgO surface roughness, and therefore device magnetoresistance, depends strongly on Ar gas pressure. Magnetoresistance of up to 236% was achieved at room temperature after thermal annealing at 425 °C and with optimal sputtering conditions. The long mean free path of target atoms at low background pressures increases their kinetic energy at the substrate surface, resulting in smooth surface morphology and correspondingly improved device performance. *© 2006 American Institute of Physics*. [DOI: 10.1063/1.2201547]

The tunneling magnetoresistance (TMR) effect in magnetic tunnel junctions (MTJs) has been extensively studied by groups with an interest in developing new types of nonvolatile magnetoresistive random-access memory (MRAM) and low-noise magnetic sensors.[1,2] The TMR ratio in conventional MTJs with an AlO_x barrier and two ferromagnetic (FM) electrode layers has generally agreed with Jullière's formula,[3] $TMR=2P_1P_2/(1-P_1P_2)$, where P_1 and P_2 are the respective spin polarizations of the two FM layers. Substantive progress has been made in improving the TMR ratio of these devices by the creation of high-quality AlO_x barriers using improved oxidation processes and by the use of electrode materials with large spin polarizations. The highest reported room temperature (RT) magnetoresistance in amorphous AlO_x-based MTJs to date has been 70% for MTJs with CoFeB electrodes.[4]

Theoretical work has shown that the use of crystalline MgO as a tunnel barrier material in MTJs could result in TMR ratios as high as 6000%, due to coherent tunneling properties predicted for this system.[5–7] First principle calculations show that the coherent tunneling of interfacial electrons with Δ_1 symmetry at the Fermi energy is the key to achieving these giant TMR ratios, and that an MgO barrier with (001) texture is required. Recently, experimental work on epitaxial Fe(001)/MgO(001)/Fe(001) MTJs grown on single crystal substrates demonstrated room temperature TMR values of up to 180%.[8–10] These MTJs exhibited good MgO (001) texture and a small lattice mismatch between Fe (001) and MgO (001). An MR ratio of 220% at RT was also achieved using polycrystalline CoFe electrodes combined with the more practical magnetron sputtering deposition method.[11] Even higher MR ratios (up to 355% at RT) were reported on a sputtered structure consisting of a highly oriented polycrystalline MgO (001) layer sandwiched by amorphous CoFeB ferromagnetic electrodes,[12–14] where the CoFeB electrodes were locally crystallized near the MgO interface during a high temperature (360 °C) annealing process.[15]

The creation of a smooth tunneling barrier is extremely important for the realization of MTJ devices with large TMR values as well as increased breakdown voltage,[16] and the smoothness of the barrier is highly dependent on MTJ deposition parameters, such as pressure. In this letter, we have systematically investigated the dependence of junction properties, including TMR ratio and roughness, on the Ar sputtering pressure. TMR ratios exceeding 200% were obtained for most junctions at optimal pressure. We also investigated the dependence of a TMR ratio on the annealing temperature (T_a), and its effect on the coercivity of the free CoFeB layer.

MTJ multilayer films were deposited on thermally oxidized Si wafers using a custom multitarget high-vacuum magnetron sputtering system (base pressure of 2×10^{-8} Torr). The MTJ stacks had the following structure (thicknesses in nanometers): substrate/Ta(30)/$Co_{50}Fe_{50}$(2)/IrMn(15)/$Co_{50}Fe_{50}$(2)/Ru(0.8)/$Co_{40}Fe_{40}B_{20}$(3)/MgO(t)/$Co_{40}Fe_{40}B_{20}$(3)/Ta(10)/Ru(5). MgO barriers with thicknesses (t) varying from 1.0 to 2.2 nm were deposited by radio frequency (RF) magnetron sputtering of an MgO target in an Ar atmosphere. The Ar pressure which was maintained during MgO sputtering was varied over the range 0.8–15 mTorr. All other metal layers were deposited by dc sputtering at a constant pressure of 1.5 mTorr. Micron-size (from 1×2 to 3×9 μm^2) elliptical junctions were patterned using standard optical lithography and ion milling. A 200-nm-thick gold layer was deposited over the defined junction area and patterned into low resistance top contact leads. After deposition, the MTJs were annealed for 1 h at temperatures ranging from 250 to 450 °C in a vacuum of 10^{-7} Torr and in an applied field of 2.5 kOe. The electrical properties of MTJs were measured at room temperature by a dc four-probe method. The TMR versus field transfer curve of a typical MTJ with a 1.6-nm-thick barrier is shown in Fig. 1. Film morphology (roughness) and crystallographic orientation were examined using an atomic force microscope (AFM) and x-ray diffraction (XRD), respectively.

[a]Electronic mail: shen@physics.brown.edu

0003-6951/2006/88(18)/182508/3/$23.00 © 2006 American Institute of Physics
Downloaded 20 Apr 2009 to 128.148.60.205. Redistribution subject to AIP license or copyright; see http://apl.aip.org/apl/copyright.jsp

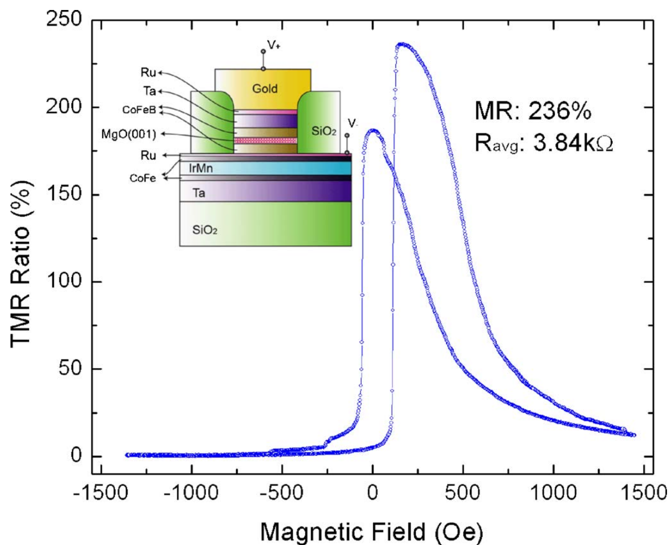

FIG. 1. (Color online) TMR curve of a typical MTJ with a 1.6-nm-thick barrier after annealing at 425 °C. The inset shows the schematic cross section of our fabricated MTJ devices.

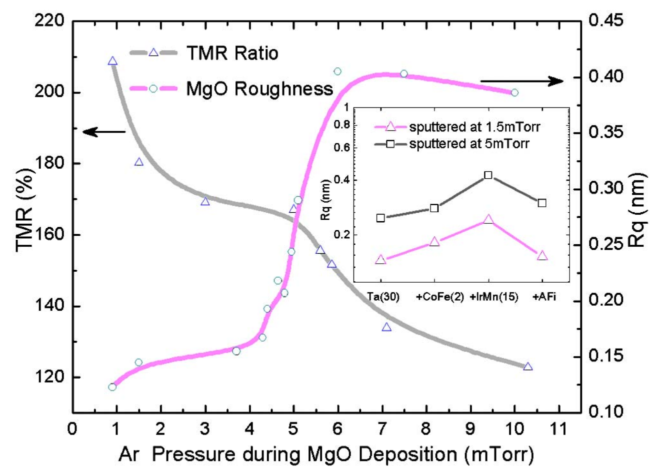

FIG. 2. (Color online)TMR ratio (triangles) and as-deposited MgO film roughness (circles) as a function of MgO sputtering pressure. R_q is the RMS roughness of the top surface of the abbreviated MTJ structure: substrate/Ta(30)/$Co_{40}Fe_{40}B_{20}$(3)/MgO(20). TMR ratios are taken from MTJs with 1.8-nm-thick MgO barriers. Inset: RMS surface roughness of each successive metal layer after deposition at two different pressures (1.5 and 5 mTorr). All thicknesses are in nanometers. The AFi layer refers to the trilayer CoFe(2)/Ru(0.8)/CoFeB(3).

The deposition of the MgO layer is the most critical step for achieving good barrier smoothness and (001) texture, which are prerequisites for large TMR values. During the MgO sputtering, the substrate holder is swept in a linear fashion above the MgO target to ensure the uniformity of the film. The target-to-wafer distance (TWD) was set to be 2 in. so as to achieve a high coating efficiency. This so-called linear dynamic deposition (LDD) technique is widely used in MRAM manufacturing, and can be used to achieve excellent thickness uniformity over large wafers.[16]

It is known that the working pressure has a significant effect on the structural properties of sputtered metal and insulator films for both dc and rf sputtering.[17] To investigate these effects for our particular system, we fabricated a number of samples with different MgO sputtering pressures. All the MTJ samples had identical layer structures as described above and an identical MgO barrier thickness (1.8 nm). We observed that the MgO deposition rate increased slowly with increasing Ar pressure, rising from 0.18 Å/s at 0.9 mTorr and reaching a maximum of 0.30 Å/s at 12 mTorr, above which the rate began to decline. This behavior can be explained by a simple molecular dynamics model. Assuming a Maxwell-Boltzmann distribution, the mean free path of a target atom traveling through the plasma can be expressed as

$$\lambda = \frac{RT}{\sqrt{2}PN\sigma}, \qquad (1)$$

where R is the universal gas constant and N is Avogadro's number. T and P are the temperature and pressure of the background gas, respectively. σ represents the cross section for scattering of the target atom off the background gas atoms, and can be considered constant over the range of sputtering pressures used. The number of collisions between sputtered atoms and argon atoms is proportional to the pressure; hence a higher pressure yields a lower mean free path. The deposition efficiency, defined as the mean number of target atoms arriving at the substrate for each incident ion which strikes the target, is then reduced as the pressure increases. However, the flux of atoms emitted from the MgO target is proportional to the pressure since there are more Ar ions impacting the target at high pressure. Taking these two trends together, it is clear that the deposition rate of MgO should reach a maximum at some intermediate pressure, similar to what we observed experimentally.

The background pressure also has a significant effect on the smoothness of the MgO film. Figure 2 shows the dependence of MgO film roughness and TMR ratio on sputtering pressure. The root mean square (RMS) roughness (R_q) at the top surface of the abbreviated MTJ stack consisting of substrate/Ta(30)/$Co_{40}Fe_{40}B_{20}$(3)/MgO(20) was evaluated using atomic force microscopy. All measurements were made with a Dimension 3100 atomic force microscope (AFM) scanning in contact mode. R_q dramatically increased with increasing pressure, with an especially large increase in the neighborhood of ~4–6 mTorr. The average TMR ratio (measured over 20 junctions for each point) is also plotted in Fig. 2, showing clearly that highest magnetoresistance is achieved at the lowest sputtering pressures. It is known that high surface mobility (kinetic energy) of sputtered atoms will result in a smooth surface morphology.[16] When a target atom is scattered by an ambient gas (Ar) atom, part of its kinetic energy will be transferred to Ar atoms. The more collisions a target atom experiences, the more energy will be lost. Therefore, the final kinetic energy of a target atom landing on the substrate is inversely proportional to the background pressure. At low pressures, more highly energetic sputtered atoms with high surface mobility reach the substrate, creating a smoother MgO film and therefore better tunneling properties. Linear sweeping of the substrate above the MgO target makes the substrate move in and out of the target atom flux, resulting in multiple-angle deposition, which further helps to improve the film smoothness and uniformity.

Low pressure deposition also significantly improved the surface smoothness of all the underlying metal layers. Inset of Fig. 2 shows the RMS surface roughness of the MTJ stack after successive metal layers were deposited at two different pressures of 1.5 mTorr (low) and 5 mTorr (high). The thickness of each layer was made identical to the full MTJ structure described earlier in this work. Low pressure (1.5 mTorr)

Downloaded 20 Apr 2009 to 128.148.60.205. Redistribution subject to AIP license or copyright; see http://apl.aip.org/apl/copyright.jsp

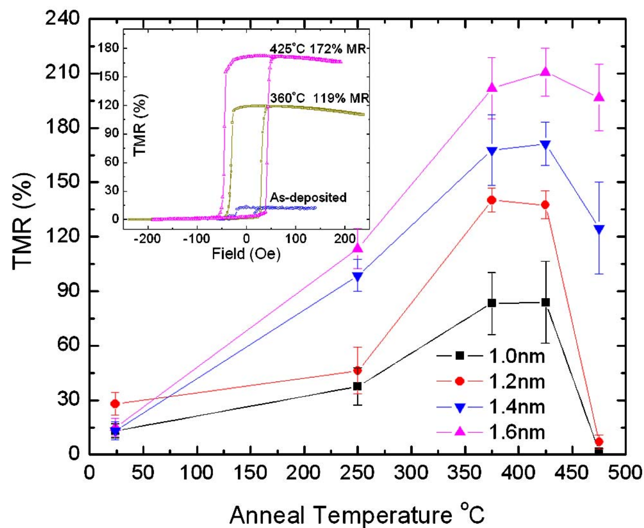

FIG. 3. (Color online) TMR ratio as a function of the annealing temperature (T_a) for four MgO barrier thicknesses: 1.0, 1.2, 1.4, and 1.6 nm. The optimal T_a was found to be between 375 and 425 °C. Inset: TMR loops of the same single MTJ (barrier thickness=1.4 nm) as deposited, after annealing at 360 °C, and after a second annealing at 425 °C.

deposition yielded consistently smoother surfaces than high pressure sputtering (the roughness was less by about a factor of two). However, in both cases it is observed that after the deposition of the CoFeB-Ru-CoFeB artificial ferrimagnet (AFi) layer the roughness was suppressed, with values decreasing almost down to the roughness of the initial Ta seed layer. This can be attributed to the amorphous nature of CoFeB, which helps to keep the film roughness at a minimum if the deposition parameters are optimized.

Figure 3 shows the TMR ratio as a function of annealing temperature (T_a) for four different MgO barrier thicknesses ranging from 1.0 to 1.6 nm. The MgO barriers measured here were all deposited at low pressure (0.9 mTorr). TMR ratios exceeding 200% were obtained for most junctions with 1.6-nm-thick barrier after thermal annealing at 425 °C, with a peak TMR value of 236%. Figure 3 shows that the TMR ratio increases dramatically with an increasing annealing temperature up to an optimum T_a between 375 and 425 °C. In order to characterize the MgO barrier behavior structurally by x-ray diffraction, we fabricated modified MTJ stacks with two changes to the above layer structure: (1) the MTJ stack was deposited as normal up until the MgO barrier, after which the deposition was discontinued and (2) in order to make the structure compatible with XRD, we deposited extra thick (100 nm) MgO layers. The resulting x-ray spectra show that the as-deposited MgO layers have a predominantly (001) polycrystalline structure [as indicated by a strong (002) diffraction peak], and that the size and shape of this peak did not significantly change after thermal annealing. The physics behind these results has been well explained by Yuasa *et al.*,[15] who showed that the as-deposited MgO layer ($\geq$5 monoatomic layers) on CoFeB has a good (001) texture, which acts as a template to crystallize the amorphous CoFeB into a (001) bcc structure when annealed above 360 °C. This effect is critical for a large TMR, as it allows the interfacial coherent tunneling of Δ_1 band electrons to dominate the TMR effect. The inset of Fig. 3 shows the TMR transfer curves of the same MTJ (barrier thickness =1.4 nm) after successive annealing at different temperatures. A sharp increase in coercivity is observed at 360 °C, with a more gradual increase in coercivity at higher temperatures. This strongly supports the conclusion that there is indeed crystallization of CoFeB into the bcc structure at the CoFeB/MgO interfaces starting at ~360 °C.

In summary, we have systematically investigated the dependence of MgO sputtering pressure on the TMR ratio in magnetic tunnel junction structures. The MgO deposition rate and kinetic energy of sputtered atoms that landed on the substrate are strongly affected by argon gas pressure in a manner which can be explained with a simple molecular dynamics model. The long mean free path experienced by target atoms at low background pressures promotes high surface mobility for the target atoms at the substrate surface, resulting in smooth surface morphology, and therefore improved magnetoresistance ratios. TMR values of up to 236% were observed at RT for MTJs with MgO barriers sputtered at low pressure (0.9 mTorr). Post-deposition thermal annealing at temperatures above 360 °C was required to obtain the highest magnetoresistance values. We observed a dramatic increase in the coercivity of the CoFeB free layer at ~360 °C, confirming the conjecture that annealing at or above this temperature promotes the crystallization of CoFeB into a bcc structure at the interface with the MgO barrier. This crystallization is critical for promoting the coherent tunneling processes which give rise to large tunnel magnetoresistance.

This work was supported by the National Science Foundation Grants Nos. DMR-0306711 and DMR05-20491.

[1] T. Miyazaki and N. Tezuka, J. Magn. Magn. Mater. **139**, L231 (1995).
[2] J. S. Moodera, L. R. Kinder, T. M. Wong, and R. Meservey, Phys. Rev. Lett. **74**, 3273 (1995).
[3] M. Jullière, Phys. Lett. **54A**, 225 (1975).
[4] D. Wang, C. Nordman, J. Daughton, Z. Qian, and J. Fink, IEEE Trans. Magn. **40**, 2269 (2004).
[5] W. H. Butler, X.-G. Zhang, T. C. Schulthess, and J. M. MacLaren, Phys. Rev. B **63**, 054416 (2001).
[6] J. Mathon and A. Umersky, Phys. Rev. B **63**, 220403 (2001).
[7] X.-G. Zhang and W. H. Butler, Phys. Rev. B **70**, 172407 (2004).
[8] J. Faure-Vincent, C. Tiusan, E. Jouguelet, F. Canet, M. Sajieddine, C. Bellouard, E. Popova, M. Hehn, F. Montaigne, and A. Schuhl, Appl. Phys. Lett. **82**, 4507 (2003).
[9] S. Yuasa, A. Fukushima, T. Nagahama, K. Ando, and Y. Suzuki, Jpn. J. Appl. Phys., Part 2 **43**, L588 (2004).
[10] S. Yuasa, T. Nagahama, A. Fukushima, Y. Suzuki, and K. Ando, Nat. Mater. **3**, 868 (2004).
[11] S. S. P. Parkin, C. Kaiser, A. Panchula, P. M. Rice, B. Hughes, M. Samant, and S.-H. Yang, Nat. Mater. **3**, 862 (2004).
[12] D. D. Djayaprawira, K. Tsunekawa, M. Nagai, H. Maehara, S. Yamagata, N. Watanabe, S. Yuasa, Y. Suziki, and K. Ando, Appl. Phys. Lett. **86**, 092502 (2005).
[13] J. Hayakawa, S. Ikeda, F. Matsukura, H. Takahashi, and H. Ohno, Jpn. J. Appl. Phys., Part 2 **44**, L587 (2005).
[14] S. Ikeda, J. Hayakawa, Y. M. Lee, R. Sasaki, T. Meguro, F. Matsukura, and H. Ohno, Jpn. J. Appl. Phys., Part 2 **44**, L1442 (2005).
[15] S. Yuasa, Y. Suzuki, T. Katayama, and K. Ando, Appl. Phys. Lett. **87**, 242503 (2005).
[16] W. Maass, B. Ocker, J. Langer, and Y. Hua, Proc. Int. Conf. on Memory Technology and Design (2005), p. 123.
[17] K. Y. Chan and B. S. Teo, J. Mater. Sci. **40**, 5971 (2005).

Downloaded 20 Apr 2009 to 128.148.60.205. Redistribution subject to AIP license or copyright; see http://apl.aip.org/apl/copyright.jsp